

## An Improved Direct Torque Control Strategy for Induction Motor Drive

<sup>1</sup>R. Zaimeddine, <sup>1</sup>L. Refoufi and <sup>2</sup>E.M. Berkouk

<sup>1</sup>Signals and Systems Research laboratory, Department of Electrical Engineering,  
University of M'hamed Bougara, Boumerdes, Algeria

<sup>2</sup>Laboratoire Commande Des Processus, Ecole National Polytechnique, El Harache, Algeria

**Abstract:** The object of this study is to study a new control structure for sensorless induction machine dedicated to electrical drives using a three-level Voltage Source Inverter (VSI). The major problem with DTC drives is the high torque ripple, to solve this problem two approaches are proposed to replace the conventional hysteresis-based controller. The output voltages of the three-level VSI can be represented by four groups: the zero voltage vectors, the small voltage vectors, the middle voltage vectors and the large voltage vectors in (d, q) plane. Then, the amplitude and the rotating velocity of the flux vector can be controlled freely. Both fast torque and optimal switching logic can be obtained. The selection is based on the value of the stator flux and the torque. Both approaches are simulated for a induction motor. The results obtained show superior performances over the conventional DTC one without need to any mechanical sensor.

**Key words:** Direct torque control, induction motor, sensorless vector control, flux estimators, switching strategy optimisation, multi-level inverter, neural-point clamped

### INTRODUCTION

The rapid development of the capacity and switching frequency of the power semiconductor devices and the continuous advance of the power electronics technology have made many changes in static power converter systems and industrial motor drive areas. The conventional GTO inverters have limitation of their dc-link voltage. Hence, the series connections of the existing GTO thyristors have been essential in realizing high voltage and large capacity inverter configurations with the dc-link voltage<sup>[1]</sup>. The vector control of induction motor drive has made it possible to be used in applications requiring fast torque control such as traction<sup>[2]</sup>. In a perfect field oriented control, the decoupling characteristics of the flux and torque are affected highly by the parameter variation in the machine.

This study describes a control scheme for direct torque and flux control of induction machines fed by a three-level inverter using a switching table. In this method, the output voltage is selected and applied sequentially to the machine through a look-up table so that the flux is kept constant and the torque is controlled by the rotating speed of the stator flux. The Direct Torque Control (DTC) is one of the actively researched control scheme which is based on the decoupled control of flux

and torque providing a very quick and robust response with a simple control construction in ac drives<sup>[3,4]</sup>. The performances permit such a system to be applicable in areas such as railway traction.

### THREE-LEVEL INVERTER TOPOLOGY AND THE NPC VOLTAGE SOURCE

Figure 1 shows the schematic diagram of Neutral Point Clamped (NPC) three-level VSI. Each phase of this inverter consists of two clamping diodes, four GTO thyristors and four freewheeling diodes. Table 1 shows the switching states of this inverter.

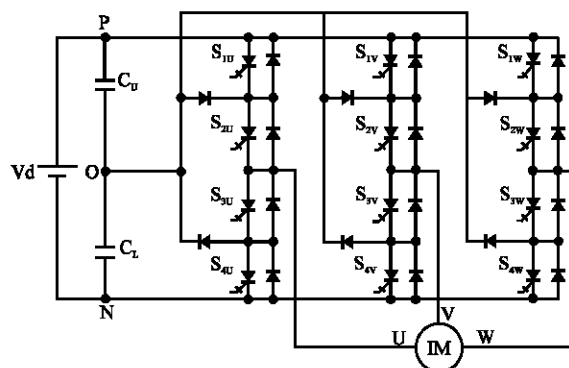


Fig. 1: Schematic diagram of a three-level GTO inverter

Table 1: Switching states of a three-level inverter

Switching states	S <sub>1</sub>	S <sub>2</sub>	S <sub>3</sub>	S <sub>4</sub>	V <sub>N</sub>
P	ON	ON	OFF	OFF	V <sub>d</sub>
O	OFF	ON	ON	OFF	V <sub>d</sub> /2
N	OFF	OFF	ON	ON	0

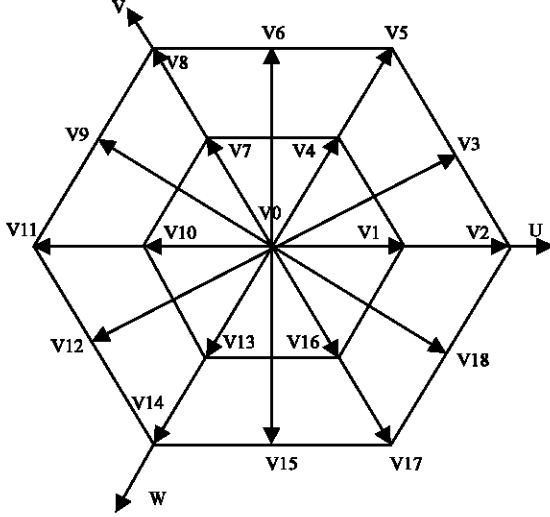


Fig. 2: Space voltage vectors of a three-level inverter

Since three kinds of switching states exist in each phase, a three level inverter has 27 switching states.

A two-level inverter is only capable to produce six non-zero voltage vectors and two zero vectors<sup>[2]</sup>.

Figure 2 shows the representation of the space voltage vectors of a three-level inverter for all switching states. According to the magnitude of the voltage vectors, we divide them into four groups: the zero voltage vectors (V<sub>0</sub>), the small voltage vectors (V<sub>1</sub>, V<sub>4</sub>, V<sub>7</sub>, V<sub>10</sub>, V<sub>13</sub>, V<sub>16</sub>), the middle voltage vectors (V<sub>3</sub>, V<sub>6</sub>, V<sub>9</sub>, V<sub>12</sub>, V<sub>15</sub>, V<sub>18</sub>), the large voltage vectors (V<sub>2</sub>, V<sub>5</sub>, V<sub>8</sub>, V<sub>11</sub>, V<sub>14</sub>, V<sub>17</sub>).

The Zero Voltage Vector (ZVV) has three switching states, the Small Voltage Vector (SVV) have two and both the Middle Voltage Vector (MVV) and the Large Voltage Vector (LVV) have only one<sup>[1]</sup>.

## INDUCTION MACHINE

Torque control of an asynchronous motor can be achieved on the basis of its model developed in a two axes (d, q) reference frame stationary with the stator winding. In this reference frame and with conventional notations (appendix), the electrical mode is described by the following equations:

$$\begin{aligned} \frac{di_{sd}}{dt} = & \frac{1}{\sigma T_r L_s} \varphi_{sd} + \frac{p\Omega}{\sigma L_s} \varphi_{sq} - \frac{1}{\sigma} \left( \frac{1}{T_r} + \frac{1}{T_s} \right) i_{sd} \\ & - p\Omega i_{sq} + \frac{1}{\sigma L_s} V_{sd} \end{aligned} \quad (1)$$

$$\begin{aligned} \frac{di_{sq}}{dt} = & -\frac{p\Omega}{\sigma L_s} \varphi_{sd} + \frac{1}{\sigma T_r L_s} \varphi_{sq} - \frac{1}{\sigma} \left( \frac{1}{T_r} + \frac{1}{T_s} \right) i_{sq} \\ & + p\Omega i_{sd} + \frac{1}{\sigma L_s} V_{sq} \end{aligned} \quad (2)$$

$$\frac{d\varphi_{sd}}{dt} = V_{sd} - R_s i_{sd} \quad (3)$$

$$\frac{d\varphi_{sq}}{dt} = V_{sq} - R_s i_{sq} \quad (4)$$

$$\varphi_{sd} = L_s i_{sd} + L_m i_{rd} \quad (5)$$

$$\varphi_{sq} = L_s i_{sq} + L_m i_{rq} \quad (6)$$

$$\varphi_{rd} = L_r i_{rd} + L_m i_{sd} \quad (7)$$

$$\varphi_{rq} = L_r i_{rq} + L_m i_{sq} \quad (8)$$

The mechanical mode associated to the rotor motion is described by:

$$J \frac{d\Omega}{dt} = \Gamma_{em} - \Gamma_r(\Omega) \quad (9)$$

$\Gamma_r \Omega$  and  $\Gamma_{em}$  are respectively the load torque and the electromagnetic torque developed by the machine.

## STATOR FLUX AND TORQUE ESTIMATION

Basically, DTC schemes require the estimation of the stator flux and torque. The stator flux evaluation can be carried out by different techniques depending on whether the rotor angular speed or (position) is measured or not. For sensorless application, the “voltage model” is usually employed<sup>[5]</sup>. The stator flux can be evaluated by integrating from the stator voltage equation.

$$\varphi_s(t) = \int (V_s - R_s I_s) dt \quad (10)$$

This method is very simple requiring the knowledge of the stator resistance only. The effect of an error in R<sub>s</sub> is usually quite negligible at high excitation frequency but becomes more serious as the frequency approaches zero<sup>[5]</sup>.

Considering the combination of states of switching functions S<sub>u</sub>, S<sub>v</sub>, S<sub>w</sub>. Fig. 3 shows the adequate voltage vector selection we can increase or decrease the stator

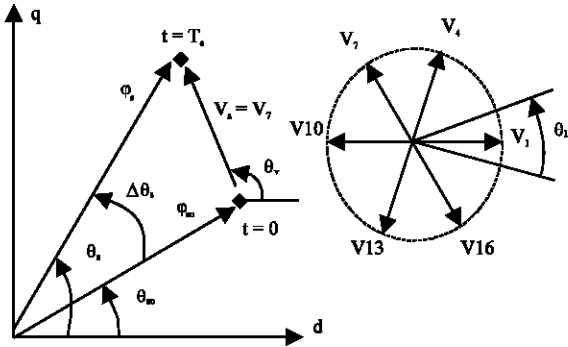


Fig. 3: Flux deviation

flux amplitude and phase to obtain the required performances. The electric torque is estimated from the flux and current information as<sup>[2]</sup>:

$$\Gamma_{em} = p(i_{sq}\phi_{sd} - i_{sd}\phi_{sq}) \quad (11)$$

**PRINCIPLE OF DIRECT TORQUE CONTROL**

Figure 4 shows a block diagram of the DTC scheme. The reference values of flux,  $\phi_s^*$  and torque,  $\Gamma_{em}^*$  are compared to their actual values and the resultant errors are fed into a two level comparator of flux and torque<sup>[2]</sup>.

The stator flux angle,  $\theta_s$ , is calculated by:

$$\theta_s = \arctan \frac{\phi_{sq}}{\phi_{sd}} \quad (12)$$

And quantified into 6 levels depending on which sector the flux vector falls into. Different switching strategies can be employed to control the torque according to whether the flux has to be reduced or increased. Each strategy affect the drive behavior in terms of torque and current ripple, switching frequency and two or four-quadrant operation capability. Assuming the voltage drop  $R_s i_s$  small, the head of the stator flux  $\phi_s$  moves in the direction of stator voltage  $V_s$  at a speed proportional to the magnitude of  $V_s$  according to

$$\Delta\phi_s = V_s T_e \quad (13)$$

The switching configuration is made step by step, in order to maintain the stator flux and torque within limits of two hysteresis bands. Where  $T_e$  is the period in which the voltage vector is applied to stator winding. Selecting step by step the voltage vector appropriately, it is then possible to drive  $\phi_s$  along a prefixed track curve.

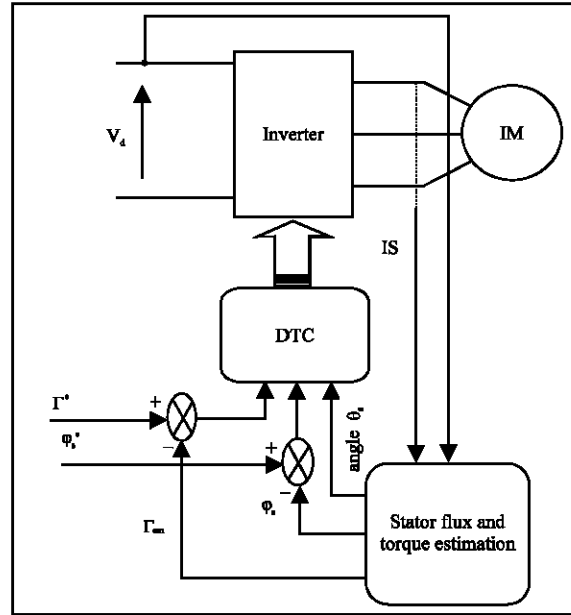


Fig. 4: Block diagram of direct torque control

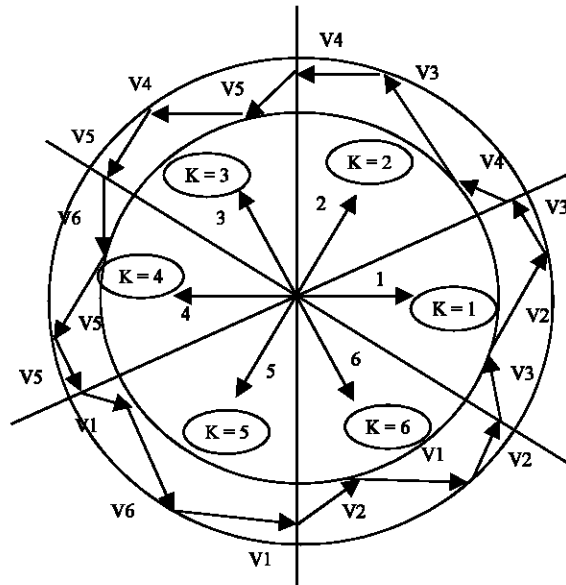


Fig. 5: Voltage vectors selection

Assuming the stator flux vector lying in the k-th sector ( $k=1,2,3,4,5,6$ ) of the ( $d, q$ ) plane, in the case of three level inverter, to improve the dynamic performance of DTC at low speed and to allow four-quadrant operation, it is necessary to involve the voltage vectors  $V_{K-1}$  and  $V_{K+2}$  in torque and flux control. In the following,  $V_{K-1}$  and  $V_{K+2}$  will be denoted “backward” voltage vectors in contraposition to “forward” voltage vectors utilised to denote  $V_{K+1}$  and  $V_{K+2}$ . A simple strategy which makes use

Table 2: Selection strategy for four-quadrant operation

	$\Gamma_{em1}$	$\Gamma_{em1}$
$\varphi_s \uparrow$	$V_{K+1}$	$V_{K-1}$
$\varphi_s \downarrow$	$V_{K+2}$	$V_{K-2}$

of these voltage vectors is shown in Table 2. The conventional DTC using three level voltage source inverter has been studied<sup>[6]</sup>.

According to this strategy, the stator flux vector is required to rotate in both positive and negative directions. By this, even at very low shaft speed, large negative values of rotor angular frequency can be achieved, which are required when the torque is to be decreased very fast. Furthermore, the selection strategy represented in Table 2 allows good flux control to be obtained even in the low speed range. However, the high dynamic performance which can be obtained utilising voltage vectors having large components tangential to the stator vector locus implies very high switching frequency.

### AN ENHANCED DIRECT TORQUE CONTROL

A switching table is used to select the best output voltage depending on the position of the stator flux and desired action on the torque and stator flux. The flux position in the (d, q) plane is quantified in twelve sectors. Alternative tables exist for specific operation mode. The switching table for the case of a two-level inverter, it is easily possible to expand the optimal vector selection to include the larger number of voltage vectors produced by three-level inverter. The appropriate vector voltage is selected in the order to reduce the number of commutation and the level of steady-state ripple.

For flux control, let the variable  $E_\varphi$  ( $E_\varphi = \varphi_s^* - \varphi_s$ ) be located in one of the three regions fixed by the constraints:

$$E_\varphi < E_{\varphi_{min}}, E_{\varphi_{min}} \leq E_\varphi \leq E_{\varphi_{max}}, E_\varphi > E_{\varphi_{max}}$$

The switable flux level is then bounded by  $E_{\varphi_{min}}$  and  $E_{\varphi_{max}}$ . The flux control is made by two-level hysteresis comparator. Three regions for flux location are noted, flux as in fuzzy control schemes, by  $E_{\varphi_n}$  (negative),  $E_{\varphi_z}$  (zero) and  $E_{\varphi_p}$  (positive).

A high level performance torque control is required. To improve the torque control let of the mismatch  $E_T$  ( $E_T = \Gamma_{em}^* - \Gamma_e$ ) to belong to one of the five regions defined by the constraints:

$$E_T < E_{T_{min2}}, E_{T_{min2}} \leq E_T \leq E_{T_{min1}}, E_{T_{min1}} \leq E_T \leq E_{T_{max1}}, E_{T_{max1}} \leq E_T \leq E_{T_{max2}} \text{ and } E_{T_{max2}} < E_T.$$

The five regions defined for torque location are also noted, as in fuzzy control schemes, by  $E_{T_{nl}}$  (negative large),  $E_{T_{ns}}$  (negative small),  $E_{T_z}$  (zero),  $E_{T_{ps}}$  (positive small),  $E_{T_{pl}}$  (positive large). The torque is then controlled by an hysteresis comparator built with two lower bounds and two upper known bounds<sup>[7]</sup>.

**Switching strategies:** The switching strategy in the order of the sector  $\theta_s$ , is illustrate by each tables. The flux and torque control by vector voltage has in nature a desecrate behavior. In fact, we can easily verify that the same vector could be adequate for a set of value of  $\theta_s$ . The number of sectors for stator flux should be as large as possible to have an adequate decision.

For this reason, we propose two approaches for direct torque control using a three-level voltage source inverter based on twelve regular sectors noted by  $\theta_1$  to  $\theta_{12}$ .

The deviation obtained as the end of the switching period  $T_e$  can be approached by the first order Taylor Seri as below.

$$\begin{aligned} \Delta\varphi_s &\approx V_s \cdot T_e \cdot \cos(\theta_v - \theta_s) \\ \Delta\theta_s &\approx T_e \cdot \frac{V_s \cdot \sin(\theta_v - \theta_s)}{\varphi_{so}} \end{aligned} \quad (14)$$

**Switching table for first approach:** In this approach, the small “backward” and “forward” voltage vectors are utilised to reduce the torque pulsation.

$\theta_1$				$\theta_2$			
$E_r \backslash E_\varphi$	Z	Z	N	$E_r \backslash E_\varphi$	Z	Z	N
PL	5	4	8	PL	5	4	8
PS	3	4	6	PS	6	7	9
ZE	0	0	0	ZE	0	0	0
NS	18	0	15	NS	18	0	15
NL	17	13	14	NL	2	16	17

$\theta_3$				$\theta_4$			
$E_r \backslash E_\varphi$	Z	Z	N	$E_r \backslash E_\varphi$	Z	Z	N
PL	8	7	11	PL	8	7	11
PS	6	7	9	PS	9	10	12
ZE	0	0	0	ZE	0	0	0
NS	3	0	18	NS	3	0	18
NL	2	16	17	NL	15	1	2

$\theta_5$				$\theta_6$			
$E_r \backslash E_\varphi$	Z	Z	N	$E_r \backslash E_\varphi$	Z	Z	N
PL	11	10	14	PL	11	10	14
PS	9	10	12	PS	12	13	15
ZE	0	0	0	ZE	0	0	0
NS	6	0	3	NS	6	0	3
NL	5	1	2	NL	8	4	5

**θ7**

$E_r \backslash E_o$	Z	Z	N
PL	14	13	17
PS	12	13	15
ZE	0	0	0
NS	9	0	6
NL	8	4	5

**θ8**

$E_r \backslash E_o$	Z	Z	N
PL	14	13	17
PS	15	16	18
ZE	0	0	0
NS	9	0	6
NL	11	7	8

**θ9**

$E_r \backslash E_o$	Z	Z	N
PL	17	16	2
PS	15	16	18
ZE	0	0	0
NS	12	0	6
NL	11	7	8

**θ10**

$E_r \backslash E_o$	Z	Z	N
PL	17	16	2
PS	18	1	3
ZE	0	0	0
NS	12	0	9
NL	14	10	11

**θ9**

$E_r \backslash E_o$	Z	Z	N
PL	17	16	2
PS	15	16	18
ZE	0	0	0
NS	12	0	9
NL	11	7	8

**θ10**

$E_r \backslash E_o$	Z	Z	N
PL	17	16	2
PS	18	1	3
ZE	0	0	0
NS	12	0	9
NL	14	10	11

**θ11**

$E_r \backslash E_o$	Z	Z	N
PL	2	1	5
PS	18	1	6
ZE	0	0	0
NS	15	0	9
NL	14	10	11

**θ12**

$E_r \backslash E_o$	Z	Z	N
PL	2	1	5
PS	3	4	6
ZE	0	0	0
NS	15	0	12
NL	17	13	14

**θ11**

$E_r \backslash E_o$	Z	Z	N
PL	2	1	5
PS	18	1	3
ZE	0	0	0
NS	15	0	12
NL	14	10	11

**θ12**

$E_r \backslash E_o$	Z	Z	N
PL	2	1	5
PS	3	4	6
ZE	0	0	0
NS	15	0	12
NL	17	13	14

**THE SIMULATION RESULTS**

The validity of the proposed techniques for three-level voltage source inverter is proved by the simulation results using Matlab-Simulink. The parameters of motors are given in the Appendix. The used flux and torque mismathes for the approach are expressed in percent with respect to th flux and torque reference values.

$$E_{\phi_{max}} = 3\%, E_{\phi_{min}} = -3\%, E_{T_{min1}} = -0.8\%, \\ E_{T_{min2}} = -3\%, E_{T_{max1}} = 0.8\%, E_{T_{max2}} = 3\%.$$

The simulation results illustrates both the steady state and the transient performance of the proposed torque control scheme. However, the machine has been supposed to run at load.

$$\Gamma_r = \left( \frac{\Gamma_{em}}{\Omega_{ref}} - K_f \right) \cdot \Omega \tag{15}$$

Figure 6 shows the torque reverse response from +9 N.m to -9 N.m and flux for 0.9 Wb. The output torque reaches the new reference torque in about 1ms, fast torque response is obtained. The response of the flux in the case of the new approach answers more quickly compared to the flux response in the conventional DTC.

Low torque ripple is observed in the Fig. 7. One nearly has the same rate of harmonic for the two approaches.

Figure 8 shows the phase current for steady state operation and the torque reverse response from +9 N.m to -9 N.m and flux for 0.9 Wb. The wave form of the stator current is closed to a sinusoidal signal.

The phase current generated by the three-level inverter has low harmonic components. Figure 9 shows the current harmonics with the new approach (7.9% THD).

**Switching table for second approach:** DTC algorithm with the small voltage vectors and zero vector are combined to ensure high-performance operation, both in the steady-state and under transient conditions.

**θ1**

$E_r \backslash E_o$	Z	Z	N
PL	5	4	8
PS	3	4	9
ZE	0	0	0
NS	18	0	12
NL	17	13	14

**θ2**

$E_r \backslash E_o$	Z	Z	N
PL	5	4	8
PS	6	7	9
ZE	0	0	0
NS	18	0	15
NL	2	16	17

**θ3**

$E_r \backslash E_o$	Z	Z	N
PL	8	7	11
PS	6	7	9
ZE	0	0	0
NS	3	0	15
NL	2	16	17

**θ4**

$E_r \backslash E_o$	Z	Z	N
PL	8	7	11
PS	9	10	12
ZE	0	0	0
NS	3	0	18
NL	15	1	2

**θ5**

$E_r \backslash E_o$	Z	Z	N
PL	11	10	14
PS	9	10	15
ZE	0	0	0
NS	6	0	18
NL	5	1	2

**θ6**

$E_r \backslash E_o$	Z	Z	N
PL	11	10	14
PS	12	13	15
ZE	0	0	0
NS	6	0	3
NL	8	4	5

**θ7**

$E_r \backslash E_o$	Z	Z	N
PL	14	13	17
PS	12	13	18
ZE	0	0	0
NS	9	0	3
NL	8	4	5

**θ8**

$E_r \backslash E_o$	Z	Z	N
PL	14	13	17
PS	15	16	18
ZE	0	0	0
NS	9	0	6
NL	11	7	8

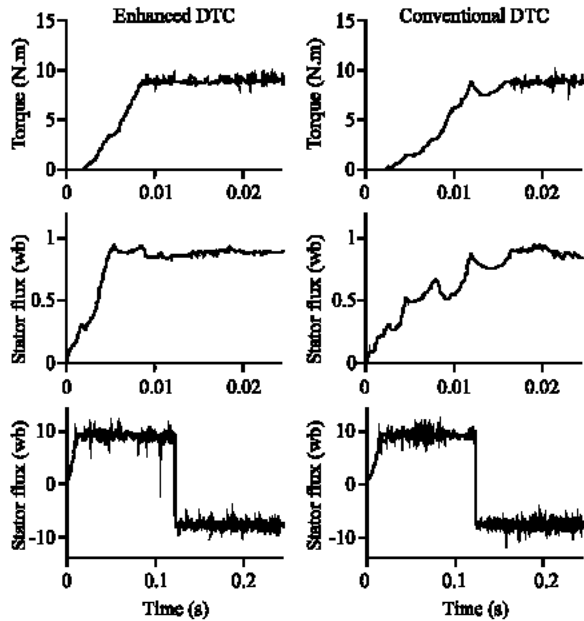


Fig. 6: Torque response and flux

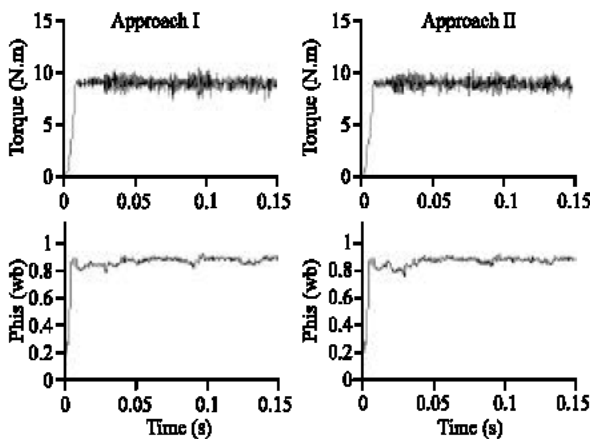


Fig. 7: Torque response and flux For steady state operation

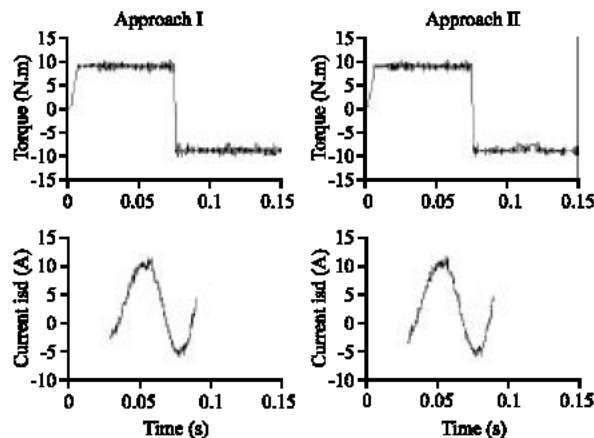


Fig. 8: Vector flux locus and current response

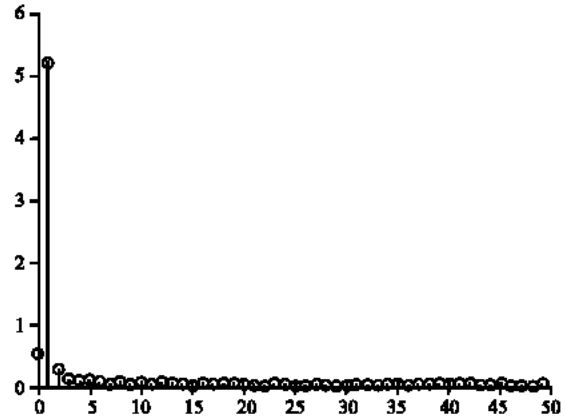


Fig. 9: Current harmonics enhanced DTC

From this analysis high dynamic performance, good stability and precision are achieved.

### CONCLUSION

The direct torque control DTC was introduced to give a fast and good dynamic torque and can be considered as an alternative to the field oriented control FOC technique. Two problems usually associated with DTC drives, which are based on hysteresis comparators, are: variable switching frequency and inaccurate stator flux estimation, which can degrade the drive performance.

The effect of proposed method has been proven by simulations. It is concluded that the proposed control produces better results for transient state operation than the conventional control.

In this paper, a DTC systems using three-level GTO voltage source inverter is presented it is suitable for high-power and high-voltage applications. We enhance the DTC approach by introducing two multi-level hysteresis comparators for flux and torque control. We impose the flux angle detection procedure by defining twelve sectors of space and establish a larger table of knowledge rules.

From the analysis of these results establish the following remarks:

The enhanced approach has a fast torque and flux response as compared to the conventional DTC. The amplitude of the torque ripples in steady state is closed for the two approaches. Comparative results demonstrate that proposed techniques preserve the DTC transient merits.

### APPENDIX

#### List of the used notations:

- s, r: indices variables
- L : magnetizing Inductance

$L_m$  : mutual inductance  
V: voltage  
i: current  
 $\phi$ : flux  
R : resistance  
 $\Gamma_{em}$  : electromagnetic torque  
J: rotor inertia  
P: number of pairs of poles  
 $\omega_s$ : statoric pulsation  
 $V_d$ : dc-link voltage  
 $K_f$ : friction Coefficient  
Te: sampling time  
E: error of the variables  
 $T_r$ : rotor time response  
 $T_s$ : stator time response.  
 $\omega_r$ : electric rotor speed,  $\Omega = p \omega_r$ .  
 $\sigma$ : leakage coefficient,  $\sigma = 1 - \frac{L_m^2}{L_s \cdot L_r}$

**Induction motors parameters:**

Rated power: 1.5 kW  
Rated voltage: 220 V  
Rated speed: 1420 rpm  
Rated frequency: 50 Hz  
Rotor resistance: 3.805  $\Omega$   
Stator inductance: 0.274 H  
Rated current : 3.64 A (Y) et 6.31 ( $\Delta$ )  
Stator resistance: 4.85  $\Omega$   
Rotor inductance: 0.274 H  
Magnetizing Inductance: 0.258 H  
Number of poles: 2  
Rotor inertia: 0.031 Kg.m<sup>2</sup>  
Friction Coefficient : 0.008 N.m.s/rd  
Vdc = 514 v  
Te =100  $\mu$ s.

**REFERENCES**

1. Lee, Y.H., B.S. Suh and D.S. Hyan, 1996. A novel PWM scheme for a three-level voltage source inverter with GTO thyristors. IEEE Trans. on Ind. Applied, pp: 260-268.
2. Takahashi, I. and T. Noguchi, 1986. A new quick-response and high-efficiency control strategy of an induction motor. IEEE Trans. on IA, pp: 820-827.
3. Trounce, J.C., S.D. Round and R.M. Duke, 2001. Comparison by Simulation of Three-level Induction Motor Torque Control Schemes for Electrical Vehicle Applications. Proc. of International Power Engineering Conference, pp: 294-299.
4. Xuezh, W.U. and L. Huang, 2001. Direct torque control of three-level inverter using neural networks as switching vector selector. IEEE IAS, annual meeting.
5. Casadei, D., G. Grandi, G. Serra and A. Tani, 1994. Switching strategies in direct torque control of induction machines. ICEM 94, pp: 204-209.
6. Zaimeddine, R. and E.M. Berkouk, 2004. A Novel DTC Scheme for a Three-level Voltage Source Inverter with GTO Thyristors. SPEEDAM, Symposium on Power Electronics, Electrical Drives, Automation and Motion, pp: F1A-9-F1A-12.
7. Bacha, F., A. Sbai and R. Dhifaoui, 1998. Tow Approaches For Direct Torque Control of an Induction Motor. CESA Symposium on control, pp: 562-568.